Click Here for Full Article

Gridded isopach maps from the South Pacific and their use in interpreting the sedimentation history of the West Antarctic continental margin

Carsten Scheuer, Karsten Gohl, and Graeme Eagles

Alfred Wegener Institute for Polar and Marine Research, Postfach 120161, D-27515 Bremerhaven, Germany (cscheuer@awi-bremerhaven.de)

[1] We model sediment isopach grids for the southern Pacific margin of West Antarctica on the basis of a compilation of more than 10,000 km of single-channel and multichannel seismic reflection data and correlations with ocean drilling sites. Following recent seismic stratigraphic models, we differentiate two main sequences, the upper of which alone is defined by seismostratigraphic indications for frequent grounded ice advances to the shelf edge off West Antarctica. The subsequent modeling of sediment thickness grids allows us to compare the pre-glacially dominated and glacially dominated sedimentary development of the study area. On the basis of available age constraints from drilling sites, we assume the onset of accumulation of sediments on the continental rise that were supplied by frequent advances of grounding ice on the continental shelf to have occurred at about 10 Ma. The thickest glacial sediment accumulations occur in front of major glacial drainage outlets, i.e., Marguerite Trough on the western Antarctic Peninsula margin, Belgica Trough in the Bellingshausen Sea, and a depression on the inner and middle shelves off Pine Island Bay in the Amundsen Sea. Glacially dominated sedimentation rates of between 140 and 170 m/m.y. are calculated for these sites.

1. Introduction

[2] The separation of Antarctica from the Australian and South American continents in Cenozoic times initiated the development of Southern Ocean currents, which were important for climate change [e.g., *Kennett*, 1977]. The opening of the Tasmanian and Drake Passage gateways were essential prerequisites for the development of the ring-shaped Antarctic Circumpolar Current (ACC), an important component of the modern oceans. This process may also have led to the gradual climatic

isolation of Antarctica [*Kennett*, 1977] and thus has been the focus of various climate model experiments investigating the glacial development of Antarctica [e.g., *Sijp and England*, 2004]. However, the opening of gateways is only one of the factors that influenced the development of circum-Antarctic currents. Several studies have shown that the ACC and Antarctic Bottom Water (AABW) are strongly guided by seafloor topography [e.g., *Lazarus and Caulet*, 1993; *Rack*, 1993]. Recent palaeobathymetric models were based on the kinematics and thermal subsidence rates of oceanic crust [e.g., *Sykes et al.*, 1998; *Brown et al.*, 2006], but lack any consideration of the effects of sediment distribution. For greater accuracy, sediment accumulations should also be taken into account in the next generation of paleobathymetric reconstructions. To do so will require gridded maps of sediment thickness.

[3] In this study, we present gridded sediment isopachs for the Pacific margin of West Antarctica. Large-scale maps of sediment thicknesses are essential prerequisites for the next generation of high-resolution paleobathymetric reconstructions. In addition, maps of sediment thicknesses on continental margins are useful for studies of terrigenous sediment supply and sediment distribution on the ocean floor. Thick sediments, deposited during glacial periods when grounded ice streams eroded the continental shelf, characterize high-latitude continental margins. These deposits provide an indirect record of glacial climate [e.g., *Cooper et al.*, 1991; *Tomlinson et al.*, 1992; *Larter et al.*, 1997; *McGinnes et al.*, 1997; *Anderson et al.*, 2001, *Rebesco et al.*, 1996]. It is possible to identify features in seismic data that are consistent with such an amplification of terrigenous sediment supply, and which can be related to the advance of grounded ice over the continental shelf to the shelf edge.

[4] In this study, we use features observed in seismic profiles to identify and map sedimentary units that formed (1) prior to advances of grounded ice on the continental shelf and (2) during later times when sediment supply was amplified due to advances of grounded ice to the shelf edge. The adoption of a date for the first development of grounded ice allows us to approximate sedimentation rates and thus make first, tentative, comparisons of local glacial sedimentation histories on the West Antarctic continental margin. Finally, comparisons of sedimentary structures on the Antarctic Peninsula and Amundsen Sea continental rises

enable some speculations on the role of bottom currents in the Amundsen Sea.

2. Data and Knowledge Base

[5] Our calculation of sediment thicknesses is based on single-channel and multichannel reflection seismic profiles acquired between 1989 and 2001. Most of the seismic data are publicly available in the digital database of the SCAR Seismic Data Library System (SDLS, available from Instituto Nazionale di Oceanografia e Geophysica Sperimentale(OGS), Trieste, Italy). Seismic data that are not yet available in digital form are not included in this study. In addition, we have taken account of drilling data from Deep Sea Drilling Project (DSDP) Leg 35 and Ocean Drilling Program (ODP) Leg 178. All the seismic profiles and the ocean drilling sites are shown in Figure. 1.

2.1. Geological Setting

[6] The highest-resolution records of Cenozoic glaciation of West Antarctica are found in the thick sediments of trough mouth fans, such as the Crary Fan in the southern Weddell Sea [e.g., *Kuvaas and Kristoffersen*, 1991] or the recently mapped Belgica fan in the Bellingshausen Sea [*Ó Cofaigh et al.*, 2005; *Scheuer et al.*, 2006a]. Thick sediments have also accumulated on the sediment mounds, channel levees, and contourite drifts that developed due to interactions between turbidity currents and along slope bottom currents [e.g., *Rebesco et al.*, 1996, 1997, 2002; *Faugères et al.*, 1999; *Nitsche et al.*, 2000].

[7] Many authors have related features observed in seismic profiles to glacial influences on terrigenous sediment input. Studies show that these features include extensive prograding sequences on the outer continental shelf, thick sediment wedges on the slope, unconformities overlain by sediment mounds or drifts on the rise, and erosional channels caused by turbidity currents [e.g., *Hampton et al.*, 1987; *Cooper et al.*, 1991, 1995; *Rebesco et al.*, 1997, 2002; *Nitsche et al.*, 2000; *Cunningham et al.*, 2002; *DeSantis et al.*, 2003]. Around much of Antarctica, where the oceanic basement is old enough, the seismic stratigraphy shows a transition to these features from earlier patterns that resemble those on nonglaciated continental margins and are therefore presumably not influenced, or far less heavily influenced, by glacial processes.

[8] In the following, we give a brief overview of the topographic setting and recent knowledge of the sedimentation processes of the area offshore of
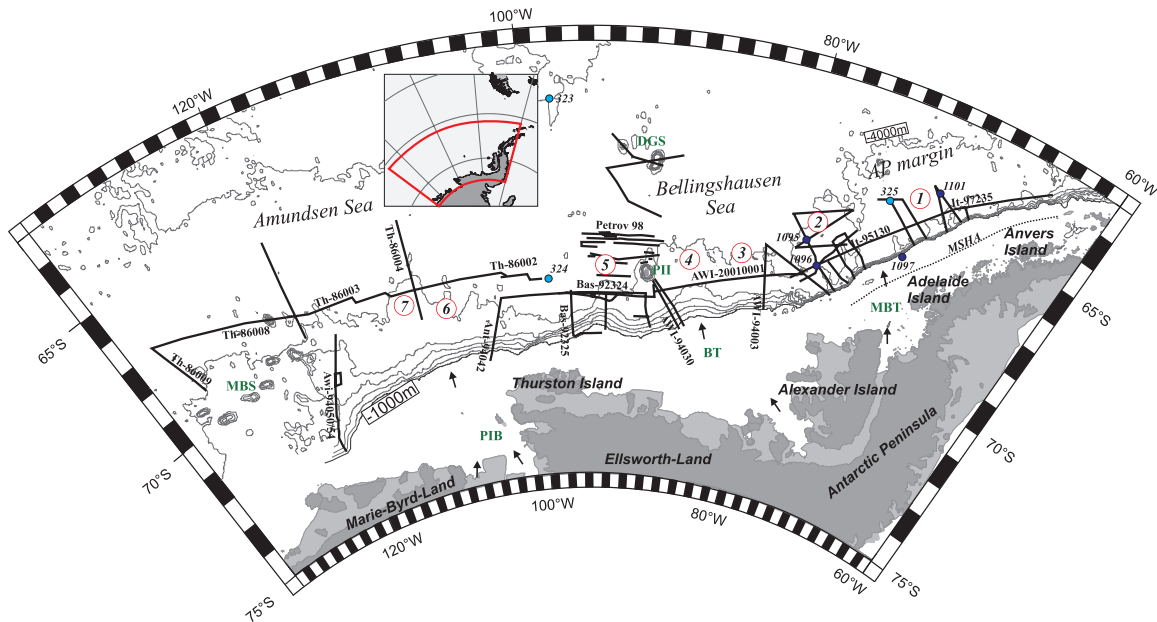
Figure 1. Overview of the South Pacific continental margin of West Antarctica, showing a network of digital available multichannel (MC) and single-channel (SC) seismic profiles (black lines) and contours of the satellite-derived predicted bathymetry from *Smith and Sandwell* [1997] (faint lines). Drill sites of DSDP Leg 35 and ODP Leg 178 are marked with black circles. Dark gray areas indicate landmasses, and medium gray indicates ice shelves. Important topographic locations are annotated. MBS, Marie Byrd Seamounts; PII, Peter I Island; DGS, DeGerlache Seamounts; PIB, Pine Island Bay; BT, Belgica Trough; MB, Marguerite Bay; MSHA, middle shelf high axis [after *Larter et al.*, 1997]. The numbers in red circles indicate the positions of some of the main sediment accumulation areas, also indicated by bathymetric contour lines. 1, drifts 3 and 4; 2, drifts 6 and 7; 3, depocenter A; 4, depocenter B; 5, depocenter C; 6, mounds Am3 and 3; 7, mound Am4.

the Antarctic Peninsula, the Bellingshausen Sea, and the Amundsen Sea.

### 2.1.1. Western Antarctic Peninsula Continental Margin

[9] A large number of seismic and bathymetric data [e.g., *Larter and Cunningham*, 1993; *Bart and Anderson*, 1995; *Rebesco et al.*, 1996, 1997, 2002; *McGinnes et al.*, 1997; *Dowdeswell et al.*, 2004; *Hernández-Molina et al.*, 2004, 2006] and the results of DSDP Leg 35, site 325 [e.g., *Hollister et al.*, 1976] and ODP Leg 178 [e.g., *Barker and Camerlenghi*, 2002] gave insights into the sedimentation history of the western Antarctic Peninsula margin (Figure 1). The interaction of a westward flowing bottom current with downslope turbidity currents led to the development of eight contourite drifts and three sediment mounds on the sides of downslope turbidity channels [e.g., *Larter and Cunningham*, 1993; *Camerlenghi et al.*, 1997; *Rebesco et al.*, 1997]. *Rebesco et al.* [1996, 1997] identified six sedimentary units, numbered M1 to M6, and related the M3/M4 boundary, where they observed amplified development of sediment drifts and the onset of erosional channels on the conti-

nental rise, to the onset of grounded ice advances on the shelf (e.g., drifts 6 and 7; Figure 2a). Ocean drilling at ODP site 1095 of Leg 178 recovered glacially transported sediment from just above the M3/M4 boundary, and dated it to 9.6 Ma, but did not reach the lower boundary of glacially influenced sediment units.

2.1.2. Bellingshausen Sea

[10] Seismic data from the Bellingshausen Sea are sparse, but allow the identification of three wide sediment depocenters on the continental slope (Figure 1). The largest, depocenter B, is interpreted as a trough mouth fan [*Ó Cofaigh et al.*, 2005; *Scheuer et al.*, 2006a]. Correlation of aggrading and prograding sequences, named units 1–3 and identified on the continental shelf/upper slope by *Nitsche et al.* [1997], with sediments on the continental rise near the easternmost depocenter, A, allowed the definition of three continental rise units, named Be1 to Be3 (e.g., Figures 2b and 2c) [*Scheuer et al.*, 2006a]. Correlation with the outer shelf units, the stratigraphy of the Antarctic Peninsula margin [*Rebesco et al.*, 1997], and ODP Leg 178 drilling results indicated that Be1 and Be2 consist predom-
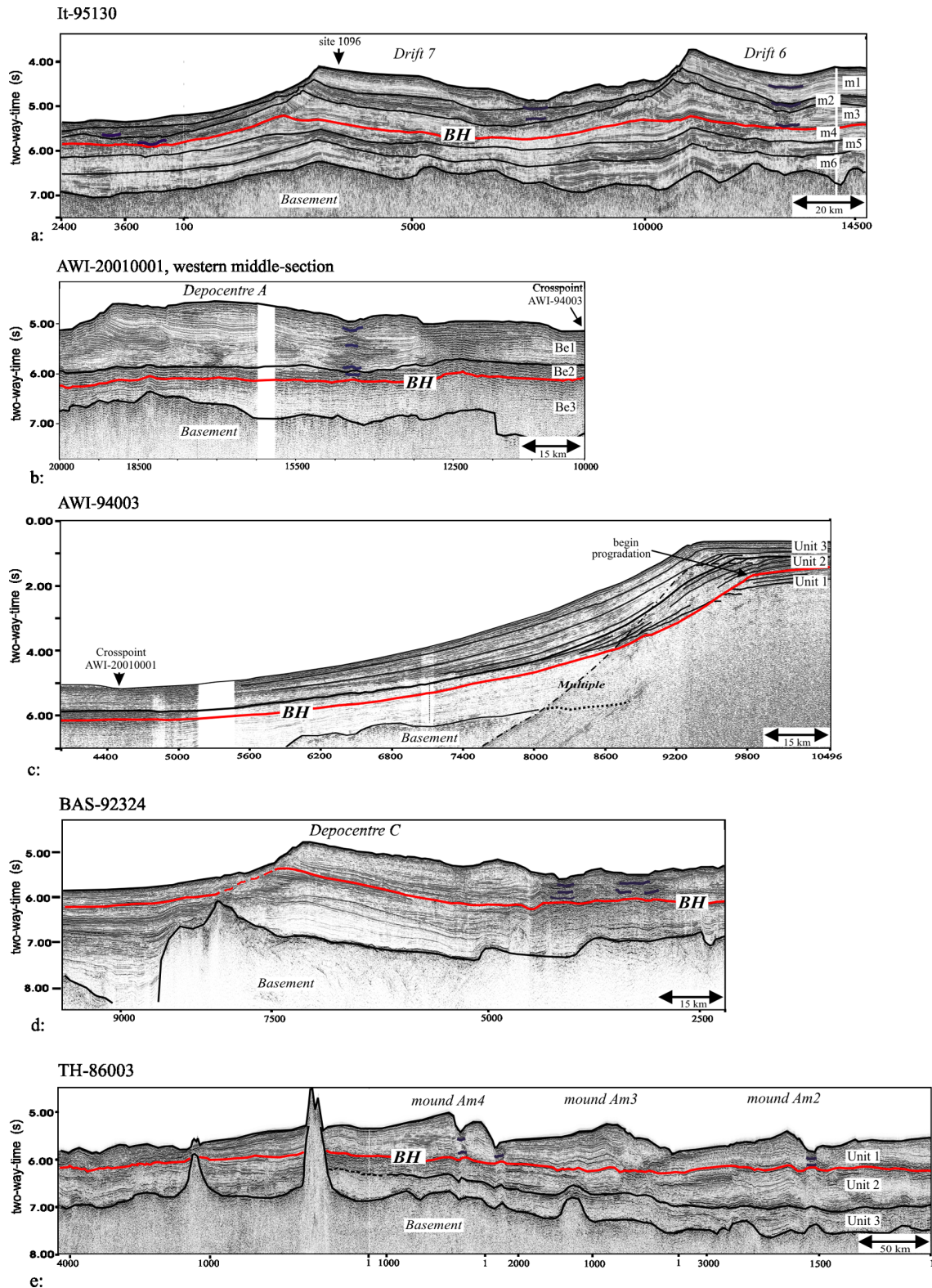
Figure 2. Interpreted line drawings of five MCS profiles on the South Pacific continental margin of West Antarctica. Interpretation of (2a) profile IT-95130 refers to *Rebesco et al.* [1997], (b and c) AWI-20010001 and AWI-94003 refers to *Scheuer et al.* [2006a], (d) BAS-92324 refers to *Cunningham et al.* [2002] and *Scheuer et al.* [2006a], and (e) TH-86003 refers to *Yamaguchi et al.* [1988]. In consideration of these interpretations we defined a boundary horizon (BH) between pre-glacially dominated and glacially dominated sediments derived from frequent grounding ice advances to the shelf edge.

inantly of glacially derived sediments, whereas the lowermost unit, Be3, developed prior to the onset of grounded ice on the shelf. No such correlation was possible for the western Bellingshausen Sea and Amundsen Sea, due to along-strike changes in the seismic stratigraphic characteristics [*Scheuer et al.*, 2006a]. Depocenter C is situated above a basement uplift at a north-south trending late Cretaceous tectonic lineation [e.g., *Gohl et al.*, 1997; *Larter et al.*, 2002] (Figure 1). On the upper continental rise, depocenter C resembles a sediment drift, but distally it has the features of a simple channel levee [*Nitsche et al.*, 1997; *Cunningham et al.*, 2002; *Scheuer et al.*, 2006a]. According to *Larter and Cunningham* [1993] and *Scheuer et al.* [2006b], the base of the drifts and channel levees indicate enhanced sediment supply to the continental rise due to advances of grounded ice to the continental shelf edge (Figure 2d).

2.1.3. Amundsen Sea

[11] The relief of the continental shelf is influenced by a large drainage outlet of the West Antarctic Ice Sheet in Pine Island Bay, which is fed by the Pine Island and Thwaites glaciers [e.g., *Vaughan et al.*, 2001; *Lowe and Anderson*, 2003; *Dowdeswell et al.*, 2006; *Evans et al.*, 2006]. Data on the continental slope and rise are scant. One seismic profile shows a prograding shelf edge [*Nitsche et al.*, 2000]. The Japan National Oil Company published seismic profiles that show several sediment mounds separated by channels in the east, and shallow basement and decreasing sediment thickness to the west, near the Marie Byrd Seamounts [*Yamaguchi et al.*, 1988] (Figures 1 and 2e). *Kimura* [1982] identified three sediment units, A, B and C, and interpreted the uppermost two, A and B, as consisting of post middle Miocene terrigenous turbidites, ice-rafted detritus and pelagic sediments. Site 323 of DSDP-Leg 35, drilled on the abyssal plain, revealed ice rafted debris in Middle Miocene sediments at a depth of approximately 300 m bsf [*Hollister et al.*, 1976].

2.2. Previous Models of Total Sediment Thicknesses

[12] The first sediment isopach maps of the South Pacific region were compiled by *Houtz et al.* [1973] and *Rodrigues et al.* [1986], based on sparse and mainly analogue seismic data acquired during early RV *Eltanin* cruises [e.g., *Tucholke and Houtz*, 1976], and on surveys related to DSDP Leg 35 [e.g., *Hollister et al.*, 1976]. *Hayes and LaBrecque* [1991] published a revised version of this sediment isopach map by adding data from more recent

seismic reflection profiles and DSDP/ODP drilling. Recently, the Hayes and LaBrecque data set was incorporated into the world isopach maps of *Laske and Masters* [1997] and *Divins* [2006]. Since publication of this second compilation, ODP Leg 178 was completed on the western Antarctic Peninsula margin [e.g., *Barker and Camerlenghi*, 2002] and new digital seismic data were acquired along the West Antarctic continental margin.

[13] *Eagles* [2006] modeled a thermally subsided South Pacific oceanic lithosphere using *Stein and Stein*'s [1992] subsidence relationship, and subtracted it from predicted bathymetry [*Smith and Sandwell*, 1997] to produce residual bathymetric anomalies. Under the assumption that most of this anomaly can be attributed to the presence of sediments on the seafloor, he used a polynomial for isostatic correction [*Sykes*, 1996] to predict total sediment thickness in the South Pacific.

3. Methods

3.1. Definition of Horizons

[14] In order to calculate sediment thicknesses and to differentiate between an upper sequence of sediments whose supply was glacially dominated and a lower sequence where glacial influence is less evident, we picked points along correlatable seismic reflections that define the seafloor, acoustic basement, and an intervening boundary horizon (BH). Reflections from the acoustic basement surface were in most cases clearly identifiable, with the exception of some of the single-channel R/V *Boris Petrov* 1998 profiles where reflection amplitudes were too low, or beneath the continental slope where seafloor multiples obscure them (Figure 1). As described in section 2.1, we used the presence or absence of certain seismic stratigraphic features as the criteria for defining the BH. For example, in the Amundsen Sea, we defined the BH at the bases of sediment mounds where we observe the initial occurrence of channels, following the interpretations of similar features on the Antarctic Peninsula margin. We interpolated the horizons through regions where low data quality, inconclusive seismic stratigraphy, or tectonic boundaries prevented correlations. After picking the horizons, we extracted their two way traveltimes (TWT [s]) at a spacing of 50 CDPs or traces.

3.2. TWT [s] to Depth [m] Conversion

[15] Sound velocities in the sediments of the Antarctic margin are sparsely known. Downhole meas-

Table 1. Comparison of Subbottom Depths, TWT, and Sound Velocities

	Subbottom Depth TWT, ms	Subbottom Depth, m	Sound Velocity, m/s
ODP Site 1095			
BH (M3/M4-boundary)	580	505	∼1740
Basement	1380[a]	1430[a]	∼2070[a]
ODP Site 1096			
BH (M3/M4-boundary)	1100[a]	950[a]	∼1730[a]
Basement	2180[a]	2155[a]	∼1980[a]
Seismic Data at CDP 1276 on Profile It-95135a[b]			
BH (M3/M4-boundary)	550	480	∼1735
Basement	1305	1286	∼1970
Seismic Data at CDP 4276 on Profile It-95130a[b]			
BH (M3/M4-boundary)	1116	1060	1900
Basement	2148	2477	2306

[a] Extrapolated.
[b] These values were calculated with the empirical formula of *Carlson et al.* [1986] using average seismic interval velocities from profiles IT-95135a (CDP 1276) and IT-95130a (CDP 4276). The comparative depth and velocities come from in situ velocity check shots on site 1095 and 1096 of ODP Leg 178 (Figure 1).

urements of velocity at ocean drilling sites are very sparse and the use of short streamers during acquisition (due to ice conditions) often precludes the generation of a reliable velocity model. The study of *Volpi et al.* [2001], for example, shows seismic interval velocities from stacking velocities that are very different to downhole velocities measured during ODP Leg 178. Because of this, we used an empirical relation [*Carlson et al.*, 1986] for the transformation of TWT [s] into depth [m], which is based on 233 correlated depths from Deep Sea Drilling Project (DSDP) data, ranging up to a depth of 1.4 s (TWT). Estimated subbottom depths (in km) are calculated using $Z = -(3.03 \pm 0.24)$ ln $[1 - (0.52 \pm 0.04) T]$ where T is two-way traveltime in [s]; the RMS error in these estimates is 26 m in depth. The method successfully reproduces the generally decreasing seismic velocity with decreasing depth and has previously been applied to seismic data acquired on the western Antarctic Peninsula and Bellingshausen Sea continental rises [*Rebesco et al.*, 1997; *Scheuer et al.*, 2006a]. A comparison of the downhole velocities in sediments above the BH at sites 1095 and 1096 of ODP Leg 178 [*Volpi et al.*, 2001] to calculated velocities shows a good agreement, and thus allows confidence in the calculated depth of the BH. The comparison also shows increasing differences with depth, as shown by the estimated and true depth of the acoustic basement (Table 1).

[16] A small number of sound velocities were determined with sonobuoys deployed along the seismic profiles TH-86002-009 in the Amundsen Sea [*Yamaguchi et al.*, 1988]. Table 2 shows comparisons of the sonobuoy data with the values calculated after *Carlson et al.* [1986]. Unfortunately, details of the sonobuoy deployments, processing method and exact parameters are not published, making it impossible to evaluate the reliability of the sonobuoy sound velocities. Furthermore, sonobuoy measurements mainly measure the horizontal velocity component, which often leads to an overestimation of velocity values, as the comparison indicates. Hence we decided to retain the sediment thicknesses calculated after *Carlson et al.* [1986] in the Amundsen Sea.

[17] The formula from *Carlson et al.* [1986] has some limitations. TWT-to-depth conversions for values higher then 1.4 s TWT are extrapolated and thus not associated with an RMS error. Furthermore, the formula becomes insolvable for values higher than 3.8 s TWT. Therefore we converted all TWT values greater than 3.0 s to depth by assuming an average velocity of 3200 m/s. This assumption affects only ∼9% of the data points of the acoustic basement horizon (Table 2), mainly observed on the continental slope/rise transition, and none of the BH picks.

3.3. Additional Input Information

[18] Because of strong seafloor multiple reflections, we were not able to define acoustic basement on most profiles crossing the continental shelf. Here, we used estimates of total sediment thickness from gravity models made along seismic profiles BAS-92325 and AWI-94003 instead [*Cunningham*

Table 2. Comparison of Depth, Sediment Thicknesses, and Sound Velocities Coming From Sonobuoy Data and Seismic Profiles, Which Were Acquired on the Continental Rise of the Amundsen Sea During the TH-86 Cruise of the RV *Hakurei-Maru*[a]

Location	Profile/ Trace	Data From Sonobuoy				Data From Seismic Profiles			
		Seafloor, m	Depth to Basement, s TWT	Sediment Thickness, m	Velocity, m/s	Seafloor, m	Depth to Basement, s TWT	Sediment Thickness, m	Velocity, m/s
SB 1	86002a/300	4280	1.57	1800	2300	4455	1.70	1792	2108
SB 2	86003a/2300	4180	2.28	3420	3000	4215	2.04	2290	2245
SB 4	86004c/2650	4560	2.01	2410	2400	4451	1.94	2124	2194
SB 7	86006/1550	4160	0.99	940	1900	4109	0.81	714	1770

[a] Sonobuoy data were read off a figure published by *Yamaguchi et al.* [1988]. The comparative data were calculated on the basis of the digital seismic profiles TH-86002-009 at the approximate sonobuoy locations, using the formula of *Carlson et al.* [1986].

et al., 2002; Alfred Wegener Institute, unpublished gravimetric data, 2001]. We exclude estimates of sediment thicknesses on the middle and inner shelf due to the lack of reliable data.

[19] In addition to this, in order to maintain a realistically smooth appearance of the grids in areas remote from seismic data control, it was necessary to include about 50 further estimates of total sediment thickness. On the continental slope and rise, our estimates were either reasonable guesses based on the physiographic context, or by comparison to the nearest seismic profile. We also referred to regional trends, but not absolute values, in the predicted sediment thickness grid of *Eagles* [2006]. As the abyssal plain is largely uncovered by newer seismic profiles, we included estimates of total sediment thicknesses from the NGDC data set, originally produced by *Hayes and LaBrecque* [1991], in the area north of 63°S and west of 80°W, sampled at 1° spacing. To us, this section of the data set appears reliable as it is based on analogue seismic profiles and results from site 323 of DSDP Leg 35 (Figures 3a and 3b).

[20] Because of discontinuous seismic reflections beneath the continental slope, we were forced to interpolate the BH along many of the cross-slope profiles. To do so, we added control points where necessary along the 1000 m bathymetric contour based on the average thickness (1800 m) of sediments above the BH where it is seen in profile crossings of this contour. On the central part of the abyssal plain, we assumed that the onset of ice rafted material, drilled in a depth of approximately 300 m at DSDP site 323, represents the distal complementary boundary to the BH horizon. We made no attempt to identify the BH beneath the

Bellingshausen Sea and western Amundsen Sea abyssal plains, where drilling data are absent.
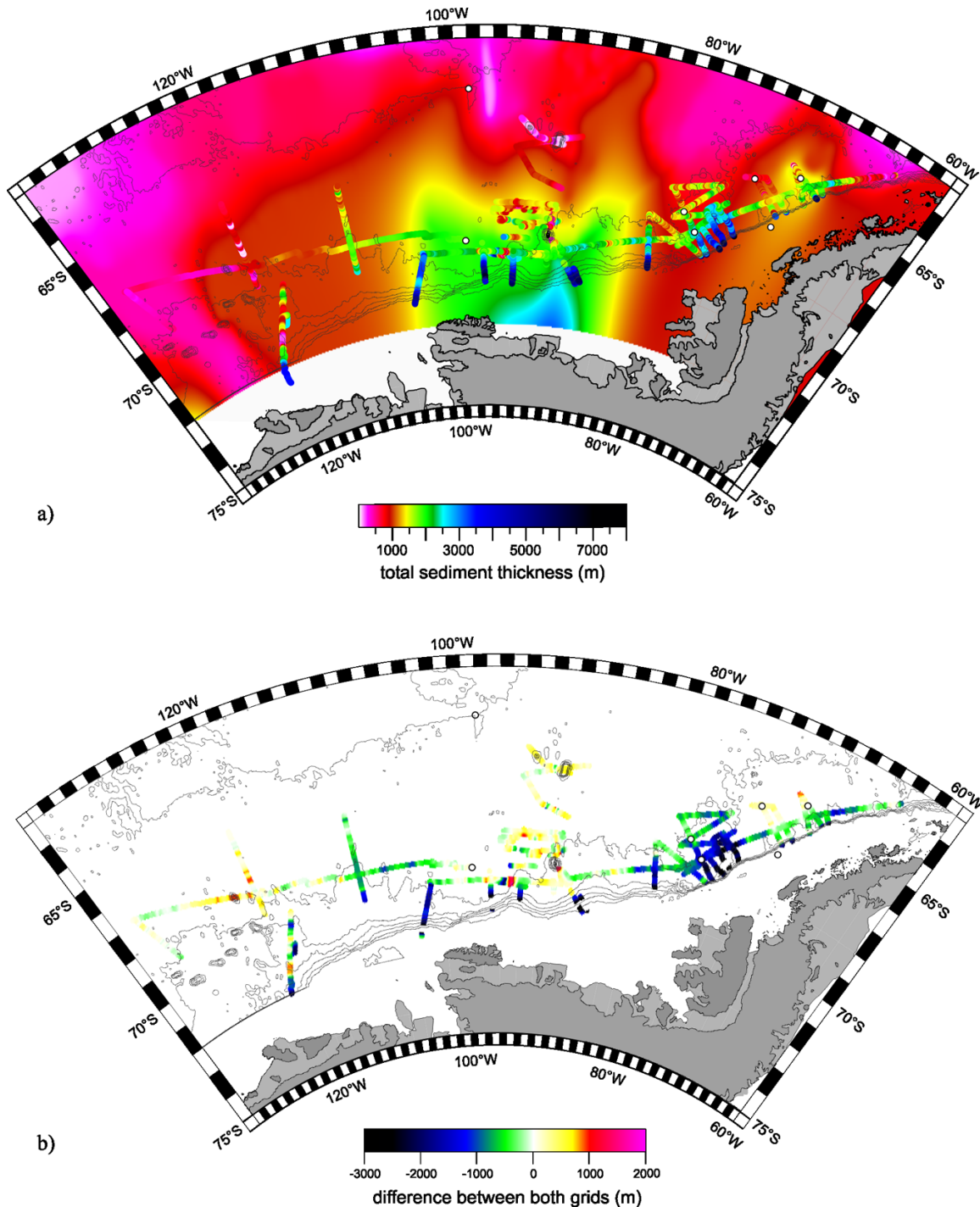
3.4. Gridding of Sediment Thicknesses

[21] We produced isopach grids of total sediment thicknesses and of thicknesses of sediments above and below the BH in the region between 60°W and 133°W and 62°S and 72°S, with a grid spacing of 2 × 2 min, using a continuous curvature gridding algorithm [*Wessel and Smith*, 2004]. We used a low tension factor in view of the large areas to be interpolated between data profiles. Before gridding, we applied a high cut cosine filter (Figure 4) to the profile data along slope in the Amundsen Sea in order to prevent short wavelength anomalies related to seamounts having an effect on the finished grid. Elsewhere, low relief of the bounding surfaces, especially the BH, means that no filtering was required.

4. Results

4.1. Total Sediment Thicknesses

[22] Figures 3a and 3b allow a comparison between the isopach grid of *Hayes and LaBrecque* [1991] and our grid of total sediment thicknesses. The Hayes and LaBrecque isopachs do not show the general trends of thick sediment accumulations on the shelf and slope, and decreasing thicknesses to the deep sea that recent cross-slope seismic profiles lend to our grid. Numerous sediment mounds, drifts and channels on the continental rise only appear in our grid. In contrast, thicknesses on the abyssal plain correspond well, as our compilation is largely based on Hayes and LaBrecque's there. Our TWT-to-depth conversion is more appropriate than that applied by Hayes and LaBrec-

Figure 3. (a) Comparison between total sediment thicknesses, based on the latest seismic data (displayed along the seismic tracks), and the isopach grid from *Divins* [2006], previously published by *Hayes and LaBrecque* [1991] (color image in the background). (b) Differences between both grids imaged along the seismic tracks.

que, who assumed an average sound velocity of 2 km/s in sediments, unless other sound velocities had been published in the original reports.

[23] Figure 5 shows some of the new observations that are possible with our grid of total sediment thickness. Peak thicknesses, exceeding 4000 m, occur along the continental shelf and slope of the entire SE Pacific continental margin, with a general decrease toward the deep sea (e.g., to 700 m at site 323, DSDP Leg 35). Sediment thicknesses on the
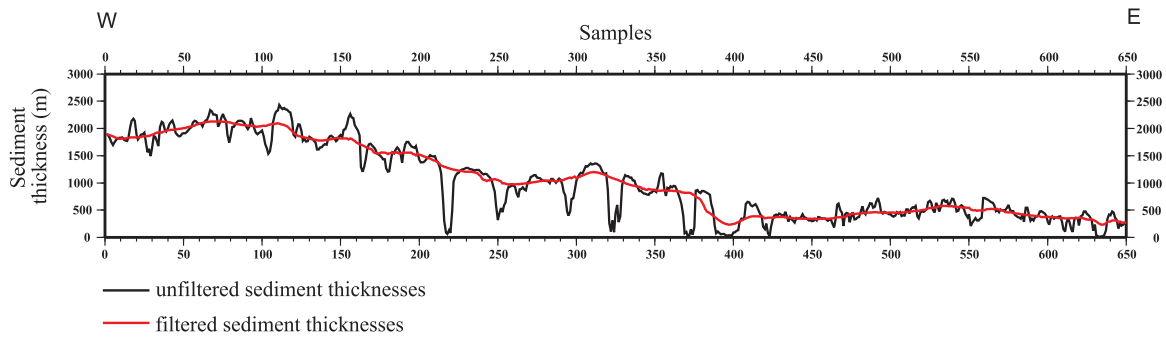
Figure 4. Filtered and unfiltered sediment thicknesses of the profiles Th-86-002/3/8/9, along-slope orientated in the Amundsen Sea. Gaussian filter with a filter width of 50 traces is used.

continental rise and abyssal plain increase from east to west. Discrete sediment mounds, drifts and wide depocenters are visible on the continental rise. Drift 3, north of Adelaide Island (thickness up to 2700 m on profile It-97235) and drifts 6 and Drift 7 (Figures 5 and 2a), north of Alexander Island (maxima of 3200 m at Drift 6 on profile It-95130) are observed on the western Antarctic Peninsula margin. Depocenters A, B and C in the Bellingshausen Sea can also be clearly identified, with thicknesses of up to 2500 m (depocenter A, Figures 5 and 2b) and 2600 m (depocenter B) on profile AWI-20010001. Depocenter C shows a north striking step in sediment thickness, downward to the west from 4500 to 450 m, which is related to the underlying basement step (profile

BAS-92324, Figures 5 and 2d). Extending northward from Peter I Island, low sediment thicknesses coincide with the basement ridge that produces the De Gerlache Gravity anomaly [*Gohl et al.*, 1997]. Profiles TH-86002 and 003 show widespread thick sediment cover in the eastern Amundsen Sea (Figures 5 and 2d). Maximum thicknesses of 2200 m are observed on profile TH-86003, and thick sediments are recorded along the northern part of profile TH-86004. To the west of this profile, sediment thicknesses show a marked decrease to less then 250 m.

[24] A comparison between our grid of total sediment thickness and that of predicted sediment thicknesses [*Eagles*, 2006] is shown on Figure 6.
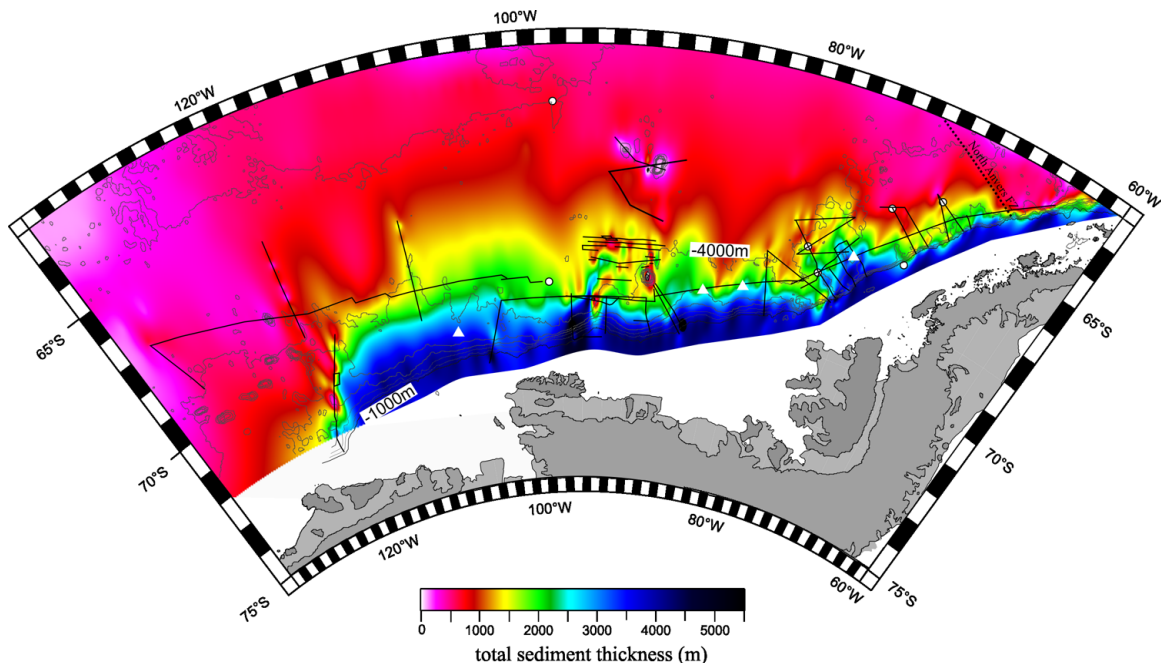
Figure 5. Isopach grid of total sediment thickness, calculated on the basis of MCS and SCS data. The faint contours indicate the satellite-derived predicted bathymetry from *Smith and Sandwell* [1997].
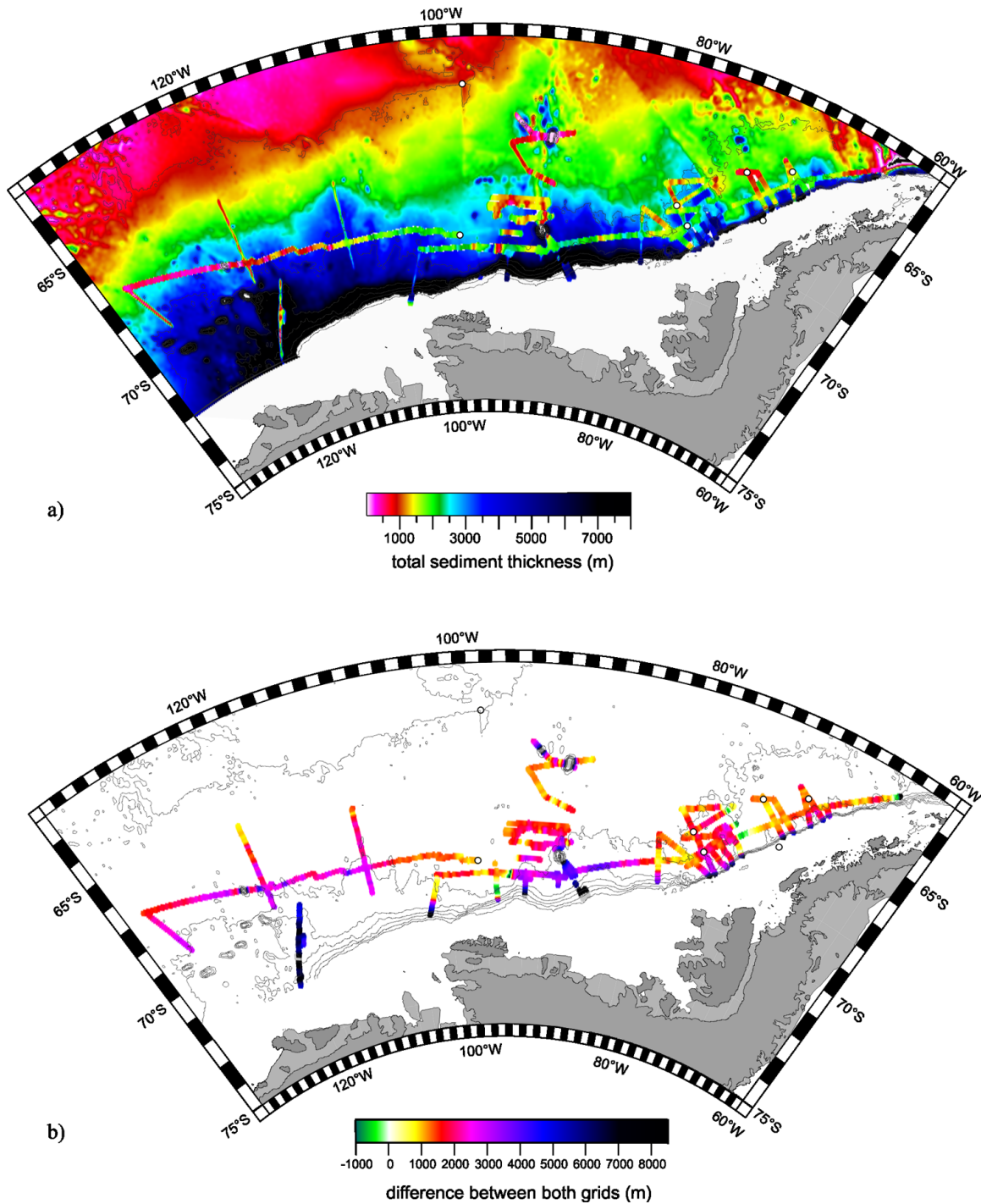
Figure 6. (a) Comparison between the total sediment thicknesses, based on the latest seismic data (displayed along the seismic tracks), and predicted sediment thicknesses derived from the grid of isostatically corrected residual bathymetry from *Eagles* [2006] (color image in the background). (b) Differences between both grids derived by subtracting the thicknesses based on seismic data from predicted sediment thicknesses, imaged along the seismic tracks.

The sediment thicknesses calculated from residual bathymetric anomalies are generally much higher than those measured in our seismic profiles. Peak differences of about 7 km occur on the upper continental slope and on the continental rise of the western Amundsen Sea. In general, the greatest differences on the continental rise, of around 2000 m, are shown in areas of high sediment
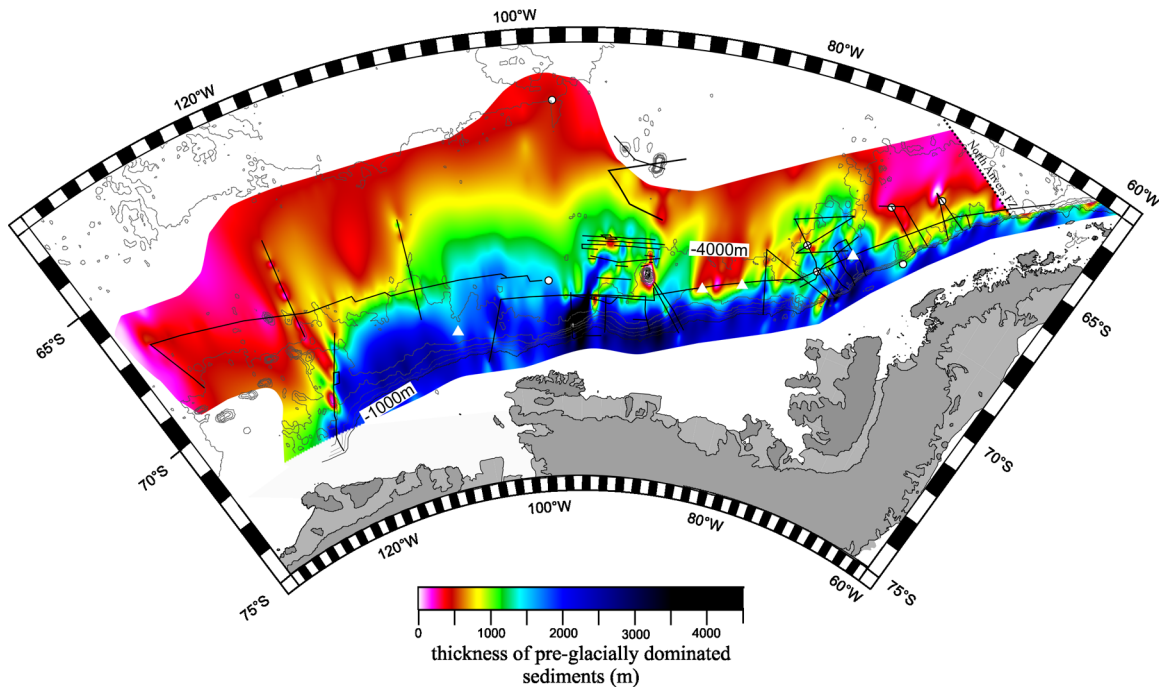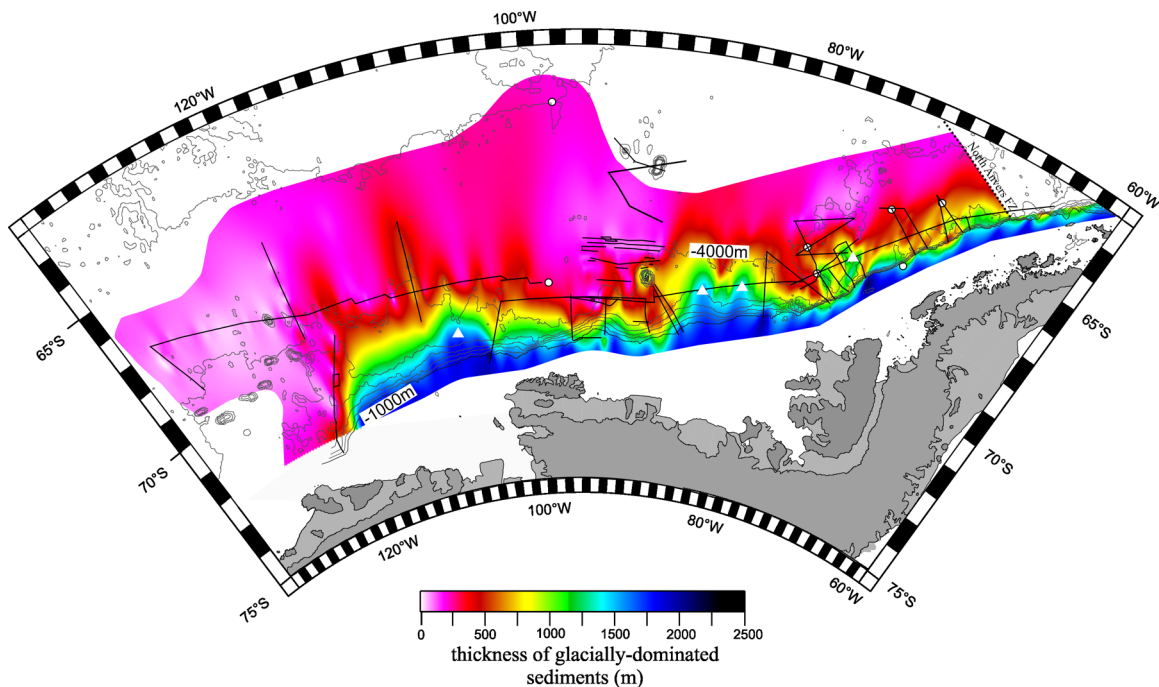
Figure 7. Isopach grid of pre-glacially dominated sediments, related to the period prior to frequent advances of grounded ice to the shelf edge. Thicknesses are calculated on the basis of MCS and SCS data. The faint contours indicate the satellite-derived predicted bathymetry from *Smith and Sandwell* [1997].

thicknesses such as at Drift 6/Drift 7. In the western Bellingshausen Sea and near Peter I Island, predicted sediment thicknesses are up to 4 km greater than seen in seismic profiles. Elsewhere, the predicted thicknesses are consistently 1–3 km greater than seismic data show.

4.2. Pre-glacially Dominated and Glacially Dominated Sediments

[25] On the continental rise, we observe an overall trend of westward increasing thicknesses in sediments above the BH (Figure 7), similar to that in the grid of total sediment thicknesses. Thicknesses of more than 1500 m occur at drifts 6 and 7, depocenters B and C, and in the eastern Amundsen Sea. Prominent basement highs, probably related to magmatic intrusions or seamounts around Peter I Island, or depressions such as that coinciding with the Bellingshausen Gravity Anomaly (sediment thicknesses exceeding 3500 m) can be clearly seen. The low thicknesses of sediments below the BH in the central Bellingshausen Sea (100–500 m), and in the western Amundsen Sea near the Marie Byrd Seamounts are conspicuous. The BH and sediments below it are not seen off the northernmost Antarctic Peninsula, where the oceanic basement is younger than 10 Ma [e.g., *Larter and Barker*, 1991; *Larter et al.*, 2002].

[26] The variability in the thickness of sediments above the BH (Figure 8) resembles that for total sediment thickness. The greatest thickness, of about 2000 m, is observed on the outer continental shelf (e.g., profile AWI-94003), and overall thicknesses decrease toward the deep sea. The thickest sediments on the continental rise are observed at the sediment depocenters, mounds and drifts (Figure 8; e.g., 1200 m at Drift 3 and 1400 m at drifts 6 and 7 on profiles IT-97235 and IT-95130). Sediment thicknesses west of Drift 7 decrease to 250 m in a wide seafloor trough. Very high thicknesses of glacial sediments are seen on depocenters A and B (up to 1500 m and 1700 m on profile AWI-20010001). Values north of profile AWI-20010001 can only be guessed at, as there are no other reliable data. We suppose these depocenters extend further out to sea than drifts 6 and 7, because of the thicker sediments above the BH and the gentler continental slope inclination. Sediment thicknesses above the BH decrease west of Peter I Island, as shown on profile BAS-92324 crossing sediment depocenter C near the continental slope (maximum thickness of 750 m). The Petrov 98 profiles indicate a strong northward decrease of sediment thicknesses above the BH to less then 200 m. However, the northernmost of these profiles, in the vicinity of the De Gerlache

Figure 8. Isopach grid of glacially dominated sediments, which we relate to amplified downslope sediment supply due to grounded ice advances on the continental shelf to the shelf edge. Thicknesses are calculated on the basis of MCS and SCS data. The faint contours indicate the satellite-derived predicted bathymetry from *Smith and Sandwell* [1997].

Seamounts, show no features that enable us to define the BH.

[27] The seismic profiles in the Amundsen Sea show sediment mounds and drifts separated by channels above the BH, similar to those on the Antarctic Peninsula margin (Figures 2a and 2e). Sediment thicknesses along profile TH-86002 and the eastern section of TH-86003 indicate four sediment mounds, which we refer to as Am1– Am4, from east to west. Profile TH-86003 shows a westward increasing trend of sediment thicknesses west of Am4. The north-south trending profile TH-86004 indicates maximum thicknesses of about 700 m and a wide northward extent of mound Am4. From here, sediment thicknesses decrease to the west.

5. Discussion

5.1. Terrigenous Sediment Supply

[28] The main reason for the overall east to west trend of increasing total and pre-glacially dominated sediment thicknesses on the continental rise and abyssal plain is the variation in the age of underlying oceanic crust, which is mostly due to diachronous cessation of oblique subduction at the continental margin. Oceanic basement ages vary from about 3 Ma on the northern Antarctic Peninsula margin to about 90–83 Ma in the Amundsen Sea. [e.g., *Barker*, 1982; *Larter and Barker*, 1991; *McCarron and Larter*, 1998; *Cunningham et al.*, 2002; *Eagles et al.*, 2004].

[29] The western shelf of the Antarctic Peninsula is divided into four major paleoice drainage basins, which during glacial times fed sediment to turbidity channels offshore and, ultimately, sediment mounds and drifts on the continental rise [e.g., *Larter et al.*, 1997; *Rebesco et al.*, 2002]. The greatest sediment thicknesses are found off these main glacial drainage areas (Figures 5 and 7), indicating that the supply of sediment by grounded ice streams during glacial periods is the primary factor for the sediment distribution on the West Antarctic continental margin. The greatest sediment thickness is observed at drifts 6 and 7, SW of Marguerite Trough, the deepest depression on the western Antarctic Peninsula continental shelf, excavated by fluctuations of paleoice streams between Alexander and Adelaide islands [e.g., *Ó Cofaigh et al.*, 2002].

[30] The topography and the development of sediment accumulations on the Bellingshausen Sea

continental margin east of Peter I Island shows some distinct differences from the western Antarctic Peninsula continental margin. Instead of several smaller turbidity channel-related sediment mounds and drifts, large depocenters have developed. Bathymetric investigations of the Bellingshausen Sea outer continental shelf revealed a wide trough named Belgica Trough, which is interpreted as the path of a major paleoice stream between Alexander and Thurston islands [*Ó Cofaigh et al.*, 2005; *Scheuer et al.*, 2006a]. Depocenter B developed seaward of this trough and thus was interpreted as a trough mouth fan by Scheuer et al., which we will refer to as the Belgica Fan. The thickness of sediments above the BH on depocenter C is low compared to those on depocenters A and B, which may indicate a lesser supply of downslope sediments on the continental margin east of Thurston Island during times of frequent grounded ice advances. Many authors interpret depocenter C as a contourite drift consisting of glacially dominated sediments built up by a westward flowing bottom current, deposited on the elevated eastern side of a basement step [e.g., *Cunningham et al.*, 1994; *Nitsche et al.*, 2000; *Scheuer et al.*, 2006b].

[31] The Amundsen Sea continental shelf is fed by two very active and fast flowing ice streams, the Pine Island and Thwaites glaciers, which account for approximately 4% of the outflow from the entire Antarctic Ice Sheet [*Vaughan et al.*, 2001]. Advances of these streams across the continental shelf during glacial maxima led to the development of glacial drainage troughs on the inner to middle shelf, of which the Pine Island Bay trough is one of the deepest (>1000 m [*Kellogg and Kellogg*, 1987; *Lowe and Anderson*, 2003]). The cross-slope profile ANT-94042 shows prograding foresets truncated by erosional unconformities [*Nitsche et al.*, 2000], through which we infer a significant supply of glacially transported sediment to the continental slope and rise. As the Pine Island Bay trough reaches the central part of the shelf in front of mound Am4 [*Lowe and Anderson*, 2003], and along-slope profiles show the highest thicknesses of sediments above the BH at mounds Am3 and Am4, we infer this area to be the main accumulation zone of glacially transported sediments.

[32] The reason for the relatively great thickness of sediments we interpreted as occurring above the BH at site 323 (about 300 m), in comparison to the northernmost RV *Petrov 98* profiles (about 200 m), may be a higher biogenic sedimentation rate. This location lies beyond the Southern ACC Front and

thus in a zone of higher organic production. However, it should be remembered that the ice rafted debris recovered near 300 m bsf at DSDP site 323 cannot be unequivocally related to the begin of grounded ice advances on the continental shelves.

5.2. Sediment Accumulation Rates

[33] The dating of the onset of grounded ice reaching the shelf edge and the accompanying amplification of large sediment accumulations such as drifts or trough mouth fans remains the subject of debate. The deepest samples of sediment drilled at site 1095, which were magnetostratigraphically dated to about 9.6 Ma [*Iwai et al.*, 2002], were deposited under glacially dominated conditions [e.g., *Barker and Camerlenghi*, 2002]. The base of glacially transported sediments was not drilled, meaning it was not possible to date the onset of grounded ice on the continental shelf reaching the shelf edge.

[34] However, drilling at ODP site 1095 just reached the boundary between *Rebesco et al.*'s [1997] seismic units M3 and M4, or our BH. This boundary indicates an important change in sediment drift development due to enhanced downslope supply of sediments, in the form of turbidity currents, which can be related to grounded ice advances on the continental shelf. Hence it may be appropriate to apply a minimum age of about 10 Ma to the BH throughout the eastern and central Bellingshausen Sea in those areas where we can correlate the M3/M4 boundary. In the western Bellingshausen Sea and Amundsen Sea, dating of the BH to 10 Ma is more speculative, as no tie to site 1095 was possible and recent studies indicate differences in the dynamic development of grounded ice reaching the shelf edge since late Miocene times [*Scheuer et al.*, 2006a].

[35] Our assumption that the BH dates everywhere to ~10 Ma is most likely an oversimplification, but it is useful because it allows us to make a coarse comparison of sedimentation histories along the West Antarctic margin. To do so, we calculated deposition rates, assuming uncompacted sediments, at locations in the four highest sediment thicknesses areas (Figures 5, 7, and 8). Of these, mound Am3 is sampled more distally, by seismic profile TH-86003, than the others. In order to calculate comparable sediment deposition rates we therefore chose a more proximal point sampled from our grid, halfway between the seismic profile and the shelf edge (Table 3).

Table 3. Average Sediment Thicknesses and Sediment Deposition Rates Calculated in the Major Accumulation Areas[a]

Location	Sediment	Deposition Period, m.y.	Sediment Thickness, m	Sediment Deposition Rate, m/m.y.
Drift 6	glacially dominated sediments	10	1400	140
Drift 6	pre-glacially dominated sediments	29	1600	55
Drift 6	total sediments	39	3000	76
Depocenter A	glacially dominated sediments	10	1550	155
Depocenter A	pre-glacially dominated sediments	37	950	26
Depocenter A	total sediments	47	2500	53
Depocenter B (eastern part)	glacially dominated sediments	10	1700	170
Depocenter B (eastern part)	pre-glacially dominated sediments	46	850	18
Depocenter B (eastern part)	total sediments	56	2550	46
Mound Am3	glacially dominated sediments	10	1600[b]	160[b]
Mound Am3	pre-glacially dominated sediments	74	1500[b]	20[b]
Mound Am3	total sediments	~85	3100[b]	36[b]

[a] We chose locations with approximately the same distance to the shelf edge in order to enable comparisons. Locations are marked by white triangles on Figures 5, 7, and 8.
[b] Sampled values from the grid.

[36] Despite the overall increase of sediment thicknesses from east to west (Figures 5, 7, and 8), we observe a decrease of the total and pre-BH sediment accumulation rates. The high rate of sedimentation below the BH off the western Antarctic Peninsula suggests a high sediment supply prior to late Miocene times. This is consistent with *Rebesco et al.*'s [1997] interpretation of seismic unit M4 (Figure 2a) as an initial drift growth stage, with an estimated onset at 15 Ma. Those authors mentioned that M4 may already have been deposited under glacial influence and in interaction with a bottom current. One explanation for this could be the mountainous nature of the Antarctic Peninsula [*Lythe et al.*, 2000]. Today, it acts as a major barrier to tropospheric circulation, resulting in high snowfall and accumulation onshore [e.g., *Reynolds*, 1981]. If this region was similarly sensitive in Miocene times, then it is possible to envisage it having responded to Miocene climate changes with earlier development of eroding ice streams than the adjacent, more flat-lying regions. Consistent with this, *Scheuer et al.* [2006a] estimated a relatively low sediment accumulation rate in the neighboring Bellingshausen Sea prior to 5.3 Ma (106 m/m.y. at depocenter A), which they attributed to the region facing a wide continental shelf with a hinterland below sea level [*Lythe et al.*, 2000]. Similar conditions apply for the Amundsen Sea, and can be invoked to explain the low accumulation rate there too.

[37] The highest accumulation rate of sediments above the BH, averaging 170 m/m.y., was estimated at depocenter B, which correlates with a peak deposition rate (295 m/m.y.) in Pliocene-Pleistocene times (since 5.3 Ma) calculated by *Scheuer et al.*

[2006a]. Those authors relate the high sedimentation rate to the development of a very large ice drainage basin (Belgica Trough), high erosion rates onshore and offshore, high ice flow velocities and the great width of the continental shelf (up to 480 km west of Alexander Island). Accumulation rates on the western Antarctic Peninsula, at depocenter A and mound Am3 are very similar, varying between 140 and 160 m/m.y. Even though sparse data in the Amundsen Sea make estimates of sediment thicknesses and accumulation rates speculative, an estimated accumulation of 160 m/m.y. on the upper continental rise seems reasonable, with respect to the similar widths of the Amundsen Sea and Bellingshausen Sea continental shelves, and the fact that Pine Island Bay is a large glacial drainage outlet.

5.3. Influence of Ocean Bottom Currents

[38] Temperature measurements [*Gordon*, 1966], seabed photography [*Hollister and Heezen*, 1967], and current meter readings [*Nowlin and Zenk*, 1988; *Camerlenghi et al.*, 1997] suggest that a westward flowing bottom contour current follows the western margin of the Antarctic Peninsula. The influence of bottom currents on the distribution of sediments and structures of sediment deposits along the West Antarctic continental margin is well documented by several studies of contourite drifts at the Antarctic Peninsula margin [e.g., *Rebesco et al.*, 1997] (Figure 2a). In addition to these, *Scheuer et al.* [2006b] identified a channel related sediment drift at depocenter C in the western Bellingshausen Sea (Figure 2d). The development of such features seems to be related to the availability of contouritic

detritus scavenged from continental slopes by frequently occurring turbidity currents.

[39] The sediment accumulations on the Antarctic Peninsula margin and in the Amundsen Sea show similarities, consisting as they do of sediment mounds with one steep and one gentle flank separated by erosional channels (Figures 2a and 2e). Although this may be taken as indicating a contour current influence in the Amundsen Sea, it should be remembered that the asymmetries of the contourite drifts on the Antarctic Peninsula margin are not always consistent with a westward current flow [*Rebesco et al.*, 2002], and so the orientations of the Amundsen Sea mounds, with their steep easterly edges, cannot be considered a strong indicator of the proposed current's direction. The higher elevation of the western channel levees may be related to the influence of the Coriolis force on turbidity currents.

5.4. Implications for Geodynamics

[40] *Eagles* [2006] noted that values in his grid of predicted sediment thicknesses (Figure 6a) were consistently greater than those in the Hayes and LaBrecque data set, and attributed this to either or both of two causes. The first cause was underestimation of sediment thicknesses by Hayes and LaBrecque due to nonimaging of seismic basement in many of their data. Although our grid confirms that the Hayes and LaBrecque data set underestimates thicknesses, the underestimation is far smaller than the difference to Eagles' predicted thicknesses. The second cause was long wavelength residual bathymetry anomalies formed due to crustal thickness variations and uplift due to flow occurring in the mantle, known as dynamic topography. *Eagles* [2006] noted that dynamic uplift of 1 km would contribute to overestimates of 3.8–6.9 km in his predicted sediment thicknesses. The regional systematic overestimate of 1–3 km in relation to our grid, shown in Figure 6b, thus suggests dynamic uplift in the range of 140–790 m affects the region.

[41] Consistent with this uplift, *Shapiro and Ritzwoller* [2004] show evidence of a peak in heat flow beneath Marie Byrd Land, which *Morelli and Danesi*'s [2004] tomographic images show is connected to a widespread low-velocity anomaly beneath the Bellingshausen and Amundsen Seas that can be interpreted in terms of warm upwelling mantle material. Dynamic topography is also often correlated with other surface manifestations of mantle convection, notably excess volcanism, for instance around Iceland [e.g., *Louden et al.*, 2004]. Studies of volcanic rocks from Marie Byrd Land

provide ample evidence for late Cenozoic volcanic activity [e.g., *Hole and LeMasurier*, 1994; *Behrendt*, 1999; *Rocchi et al.*, 2002]. Offshore, in the Amundsen Sea, there is further evidence for excess volcanism at the Marie Byrd Seamounts, although seismic data and subsidence calculations on guyots suggest this occurred in Paleogene times. Peter I Island, further east, is an active volcano that may also be attributed, along with the nearby De Gerlache seamounts, to the same cause as the regional uplift. The peak sediment thickness overestimates in *Eagles'* [2006] grid coincide with these centers and thus may be related to increased dynamic topography around them, or to crustal thickening associated with the volcanic activity.

5.5. Outlook

[42] The interpolated sediment isopach grids can be used to adjust existing paleobathymetric models for the effects of sedimentation. Such grids should be a central element of paleoceanographic models that set out to investigate the origins and effects of topographically steered currents like the ACC or AABW. To do this for the various times that might be of interest in the region will require the classification of the entire sediment package into discrete dated sediment units. As yet, the sparse data acquired in the study area do not allow the establishment of such a classification. The lack of data coming from deep penetrating ocean boreholes in the Amundsen Sea makes a dating of sediment units there especially difficult. Our coarse classification into pre-glacially dominated and glacially dominated sediments along seismic profiles and its northward extrapolation is the first classification of the sediments ranging across the South Pacific. Our assumption that these sequences are separated by an isochronous surface, BH, is an oversimplification, but it enables a first tentative comparison of sedimentation histories along the West Antarctic margin which can be used to guide future data acquisition efforts.

6. Summary and Conclusions

[43] A large set of seismic reflection data acquired in the Southern Pacific off West Antarctica is used to model isopach grids that provide insights into the tectonic structure and sedimentary architecture of the study area. In the future, grids like these can be used to improve existing paleobathymetric models by considering the effects of sedimentation, in order to provide more precise boundary conditions for models of paleoceanographic develop-

ment. The approximation of an age of about 10 Ma for the boundary between predominantly nonglacial related sediments and those supplied due to the advances of grounded ice on the continental shelf allows approximations of sedimentation rates on the continental rise and thus a comparison of local sedimentation histories.

[44] In comparison to the Bellingshausen and Amundsen Seas, high sedimentation rates on the western margin of the Antarctic Peninsula prior to 10 Ma can be related to the elevated topography of the Antarctic Peninsula hundreds of meters above sea level. This topography presented a source of terrigenous sediments that was missing from most other parts of West Antarctica, and may have promoted weather patterns that gave rise to the earlier development of ice streams that transported sediment to the continental rise. In contrast, preglacial sediment accumulation rates in the Bellingshausen Sea and Amundsen Sea are about half as much as on the Antarctic Peninsula, which can be related to low relief of the sediment source area, most of which lies below sea level.

[45] The distribution of glacially dominated sediments on the continental rise is, in general, consistent with the arrangement of recent drainage outlets on the shelf, as the thickest deposits were identified at the mouths of the Marguerite Trough (Antarctic Peninsula), Belgica Trough (Bellingshausen Sea) and in the central Amundsen Sea. Maximum sedimentation of glacially dominated sediments is estimated in the western Bellingshausen Sea and central Amundsen Sea.

[46] However, differences in sediment accumulation rates suggest significant local variability in the timing of glaciations and ice advances over the West Antarctic continental margin. So, we reiterate the tentative nature of our classification, which is due to sparse coverage of seismic profiles and very limited or absent drill hole information.

Acknowledgments

References

Anderson, J. B., J. S. Wellner, A. L. Lowe, A. B. Mosola, and S. S. Shipp (2001), The footprint of the expanded West Antarctic Ice Sheet: Ice stream history and behavior, *GSA Today*, *11*, 4–9.

Barker, P. F. (1982), The Cenozoic subduction history of the Pacific margin of the Antarctic Peninsula: Ridge crest interactions, *J. Geol. Soc. London*, *139*, 787–801.

Barker, P. F., and A. Camerlenghi (2002), Glacial history of the Antarctic Peninsula from Pacific margin sediments [online], *Proc. Ocean Drill. Program Sci. Results*, *178*, 40 pp. (Available at http://www-odp.tamu.edu/publications/178_SR/synth/synth.htm)

Bart, P. J., and J. B. Anderson (1995), Seismic record of glacial events affecting the Pacific margin of the northwestern Antarctic Peninsula, in *Geology and Seismic Stratigraphy of the Antarctic Margin*, *Antarct. Res. Ser.*, vol. 68, edited by A. K. Cooper, P. F. Barker, and G. Brancolini, pp. 75–95, AGU, Washington, D. C.

Behrendt, J. C. (1999), Crustal and lithospheric structure of the West Antarctic Rift System from geophysical investigations—A review, *Global Planet. Change*, *23*, 25–44.

Brown, B., C. Gaina, and R. D. Müller (2006), Circum-Antarctic palaeobathymetry: Illustrated examples from Cenozoic to recent times, *Palaeogeogr. Palaeoclimatol. Palaeoecol.*, *231*, 158–168, doi:10.1016/j.palaeo.2005.07.033.

Camerlenghi, A., A. Crise, C. J. Pudsey, E. Accerboni, R. Laterza, and M. Rebesco (1997), Ten-month observation of the bottom current regime across a sediment drift of the Pacific margin of the Antarctic Peninsula, *Antarct. Sci.*, *9*, 426–433.

Carlson, R. L., A. F. Gangi, and K. R. Snow (1986), Empirical reflection travel time versus depth and velocity versus depth functions for the deep sea sediment column, *J. Geophys. Res.*, *91*, 8249–8266.

Cooper, A. K., P. Barrett, K. Hinz, V. Traubea, G. Leitchenkov, and H. Stagg (1991), Cenozoic prograding sequences of the Antarctic continental margin: A record of glacioeustatic and tectonic events, *Mar. Geol.*, *102*, 175–213.

Cooper, A. K., P. F. Barker, and G. Brancolini (1995), *Geology and Seismic Stratigraphy of the Antarctic Margin*, *Antarct. Res. Ser.*, vol. 68, 301 pp., AGU, Washington, D. C.

Cunningham, A. P., R. D. Larter, and P. F. Barker (1994), Glacially prograded sequences on the Bellingshausen Sea continental margin near 90°W, *Terra Antart.*, *1*, 267–268.

Cunningham, A. P., R. D. Larter, P. F. Barker, K. Gohl, and F.-O. Nitsche (2002), Tectonic evolution of the pacific margin of Antarctica: 2. Structure of Late Cretaceous–early Tertiary plate boundaries in the Bellingshausen Sea from seismic reflection and gravity data, *J. Geophys. Res.*, *107*(B12), 2346, doi:10.1029/2002JB001897.

DeSantis, L., G. Brancolini, and F. Donda (2003), Seismostratigraphic analysis of the Wilkes Land continental margin (East Antarctica): Influence of glacially driven processes on the Cenocoic deposition, *Deep Sea Res., Part II*, *50*, 1563–1594.

Divins, D. L. (2006), NGDC Total Sediment Thickness of the World's Oceans & Marginal Seas, Total Sediment Thickness of the World's Oceans and Marginal Seas, http://www.ngdc.noaa.gov/mgg/sedthick/sedthick.html, Natl. Geophys. Data Cent., Boulder, Colo.

Dowdeswell, J. A., C. Ó. Cofaigh, and C. J. Pudsey (2004), Continental slope morphology and sedimentary processes at the mouth of an Antarctic palaeo-ice stream, *Mar. Geol.*, *204*, 203–214.

Dowdeswell, J. A., J. Evans, C. Ó. Cofaigh, and J. B. Anderson (2006), Morphology of the continental slope off Pine Island Bay, Amundsen Sea, West Antarctica, *Bull. Geol. Soc. Am.*, *118*(5), 606–619.

Eagles, G. (2006), Deviations from an ideal thermal subsidence surface in the southern Pacific Ocean, in *Frontiers*

in Antarctic Earth Sciences, Terra Antart. Rep. 12, pp. 109–118, Terra Antart. Publ., Siena, Italy.

Eagles, G., K. Gohl, and R. D. Larter (2004), High-resolution animated tectonic reconstruction of the South Pacific and West Antarctic margin, *Geochem. Geophys. Geosyst.*, 5, Q07002, doi:10.1029/2003GC000657.

Evans, J., J. A. Dowdeswell, C. Ó. Cofaigh, J. B. Anderson, and T. J. Benham (2006), Extent and dynamics and processes of the West Antarctic ice sheet on the outer continental shelf of Pine Island Bay during the last glaciation, *Mar. Geol.*, 230, 1–2, 53–72.

Faugères, J. C., D. A. D. Stow, P. Imbert, and A. Viana (1999), Seismic features diagnostic of contourite drifts, *Mar. Geol.*, 162, 1–38.

Gohl, K., F. Nitsche, and H. Miller (1997), Seismic and gravity data reveal Tertiary interplate subduction in the Bellingshausen Sea, southeast Pacific, *Geology*, 25, 371–374.

Gordon, A. L. (1966), Potential temperature, oxygen and circulation of bottom water in the Southern Ocean, *Deep Sea Res.*, 13, 1125–1138.

Hampton, M. A., S. L. Eittreim, and B. M. Richmond (1987), Post-breakup sedimentation on the Wilkes Land Margin, Antarctica, in *The Antarctic Continental margin, Geology and Geophysics of Offshore Wilkes Land, Earth Sci. Ser.*, vol. 5A, edited by S. L. Eittreim and M. A. Hampton, pp. 75–89, Circum-Pac. Counc. for Energy and Miner. Recour., Reston, Va.

Hayes, D. E., and J. L. LaBrecque (1991), Sediment isopachs: Circum-Antarctic to 30°S, in *Marine Geological and Geophysical Atlas of the Circum-Antarctic to 30°S, Antarct. Res. Ser.*, vol. 54, edited by D. E. Hayes, pp. 29–33, AGU, Washington, D. C.

Hernández-Molina, F. J., R. D. Larter, M. Rebesco, and A. Maldonado (2004), Miocene changes in bottom current regime recorded in continental rise sediments on the continental margin of the Antarctic Peninsula, *Geophys. Res. Lett.*, 31, L22606, doi:10.1029/2004GL020298.

Hernández-Molina, F. J., R. D. Larter, M. Rebesco, and A. Maldonado (2006), Miocene reversal of bottom water flow along the Pacific Margin of the Antarctic Peninsula: Stratigraphic evidence from a contourite sedimentary tail, *Mar. Geol.*, 228, 93–116, doi:10.1016/j.margeo.2005.12.010.

Hole, M. J., and W. E. LeMasurier (1994), Tectonic controls on the geochemical composition of Cenozoic alkali basalts from West Antarctica, *Contrib. Mineral. Petrol.*, 117, 187–202.

Hollister, C. D., and B. C. Heezen (1967), The floor of the Bellingshausen Sea, in *Deep-Sea Photography, Johns Hopkins Oceanogr. Stud.*, vol. 3, edited by J. B. Hersey, pp. 177–189, Johns Hopkins Press, Baltimore, Md.

Hollister, C. D., et al. (1976), *Initial Reports of Deep Sea Drilling Project*, vol. 35, 929 pp., U.S. Gov. Print. Off., Washington, D. C.

Houtz, R. E., M. Ewing, D. E. Hayes, and B. Naini (1973), Sediments isopachs in the Indian and Pacific sector (105°E to 70°W), *Antarct. Map Folio Ser., Folio 17*, Plate 5.

Iwai, M., G. D. Acton, D. Lazarus, L. E. Osterman, and T. Williams (2002), Magnetobiochronologic synthesis of ODP Leg 178 rise sediments from the Pacific sector of the Southern Ocean: Sites 1095, 1096 and 1101, *Proc. Ocean Drill. ProgramSci. Results* [CD-ROM], 178, 1–40.

Kellogg, T. B., and D. E. Kellogg (1987), Recent glacial history and rapid ice stream retreat in the Amundsen Sea, *J. Geophys. Res.*, 92, 8859–8864.

Kennett, J. P. (1977), Cenozoic evolution of Antarctic glaciation, the circum-Antarctic Ocean, and their impact on global paleoceanography, *J. Geophys. Res.*, 82, 3843–3860.

Kimura, K. (1982), Geological and geophysical survey in the Bellingshausen Basin, off Antarctica, *Antarct. Rec.*, 75, 12–24.

Kuvaas, B., and Y. Kristoffersen (1991), The Crary Fan: A trough-mouth fan on the Weddell Sea continental margin, Antarctica, *Mar. Geol.*, 97, 345–362.

Larter, R. D., and P. F. Barker (1991), Effects of ridge crest-trench interaction on Antarctic-Phoenix spreading forces on a young subducting plate, *J. Geophys. Res.*, 96, 19,583–19,608.

Larter, R. D., and A. P. Cunningham (1993), The depositional pattern and distribution of glacial-interglacial sequences on the Antarctic Peninsula Pacific margin, *Mar. Geol.*, 109, 203–219.

Larter, R. D., M. Rebesco, L. E. Vanneste, L. A. P. Gamboa, and P. F. Barker (1997), Cenozoic tectonic, sedimentary and glacial history of the continental shelf west of Graham Land, Antarctic Peninsula, in *Geology and Seismic Stratigraphy on the Antarctic Margin*, part 2, *Antarct. Res. Ser.*, vol. 71, edited by A. K. Cooper and P. F. Barker, pp. 1–27, AGU, Washington, D. C.

Larter, R. D., A. P. Cunningham, P. F. Barker, K. Gohl, and F.-O. Nitsche (2002), Tectonic evolution of the Pacific margin of Antarctica: 1 Late Cretaceous tectonic reconstructions, *J. Geophys. Res.*, 107(B12), 2345, doi:10.1029/2000JB000052.

Laske, G., and G. Masters (1997), A global digital map of sediment thickness, *Eos Trans. AGU*, 78(46), Fall Meet. Suppl., F483.

Lazarus, D., and J.-P. Caulet (1993), Cenozoic Southern Ocean reconstruction from sedimentologic, radiolarian, and other microfossil data, in *The Antarctic Paleoenvironment: A Perspective on Global Change, Antarct. Res. Ser.*, vol. 56, edited by L.-P. Kennet and D. A. Warnke, pp. 145–174, AGU, Washington, D. C.

Louden, K. E., B. E. Tucholke, and G. N. Oakey (2004), Regional anomalies of sediment thickness, basement depth and isostatic crustal thickness in the North Atlantic Ocean, *Earth Planet. Sci. Lett.*, 224, 193–211.

Lowe, A. L., and J. B. Anderson (2003), Evidence for abundant subglacial meltwater beneath the paleo-ice sheet in Pine Island Bay, Antarctica, *J. Glaciol.*, 49(164), 125–138.

Lythe, M. B., D. G. Vaughan, and the BEDMAP Consortium (2000), BEDMAP–Bed topography of the Antarctic, scale 1:10,000,000, Br. Antarct. Surv., Cambridge, U.K.

McCarron, J. J., and R. D. Larter (1998), Late Cretaceous to early Tertiary subduction history of the Antarctic Peninsula, *J. Geol. Soc. London*, 155, 255–268.

McGinnes, J. P., D. E. Hayes, and N. W. Driscoll (1997), Sedimentary processes across the continental rise of the southern Antarctic Peninsula, *Mar. Geol.*, 141, 91–109.

Morelli, A., and S. Danesi (2004), Seismological imaging of the Antarctic continental lithosphere: A review, *Global Planet. Change*, 42, 155–165.

Nitsche, F. O., K. Gohl, K. Vanneste, and H. Miller (1997), Seismic expression of glacially deposited sequences in the Bellingshausen and Amundsen Seas, West Antarctica, in *Geology and Seismic Stratigraphy of the Antarctic Margin*, part 2, *Antarct. Res. Ser.*, vol. 71, edited by P. F. Barker and A. K. Cooper, pp. 95–108, AGU, Washington, D. C.

Nitsche, F. O., A. P. Cunningham, R. D. Larter, and K. Gohl (2000), Geometry and development of glacial continental margin depositional systems in the Bellingshausen Sea, *Mar. Geol.*, 162, 277–302.

Nowlin, W. D.Jr., and W. Zenk (1988), Currents along the margin of the South Shetland Island Arc, *Deep Sea Res.*, 35, 805–833.

Ó Cofaigh, C., C. J. Pudsey, J. A. Dowdeswell, and P. Morris (2002), Evolution of subglacial bedforms along a paleo-ice stream, Antarctic Peninsula continental shelf, *Geophys. Res. Lett.*, *29*(8), 1199, doi:10.1029/2001GL014488.

Ó Cofaigh, C., R. D. Larter, J. A. Dowdeswell, C.-D. Hillenbrand, C. J. Pudsey, J. Evans, and P. Morris (2005), Flow of the West Antarctic ice sheet on the continental margin of the Bellingshausen Sea at the Last Glacial Maximum, *J. Geophys. Res.*, *110*, B11103, doi:10.1029/2005JB003619.

Rack, F. R. (1993), A geologic perspective on the Miocene evolution of the Antarctic Circumpolar Current system, *Tectonophysics*, *222*, 397–415.

Rebesco, M., R. D. Larter, A. Camerlenghi, and P. F. Barker (1996), Giant sediment drifts on the continental rise west of the Antarctic Peninsula, *Geo Mar. Lett.*, *16*, 65–75.

Rebesco, M., R. D. Larter, P. F. Barker, A. Camerlenghi, and L. E. Vanneste (1997), History of sedimentation on the continental rise west of the Antarctic Peninsula, in *Geology and Seismic Stratigraphy on the Antarctic Margin*, part 2, *Antarct. Res. Ser.*, vol. 71, edited by A. K. Cooper and P. F. Barker, pp. 29–49, AGU, Washington, D. C.

Rebesco, M., C. J. Pudsey, M. Canals, A. Camerlenghi, P. F. Barker, F. Estrada, and A. Giorgetti (2002), Case study 27: Sediment drifts and deep-sea channel systems, Antarctic Peninsula Pacific margin, mid-Miocene to present, in *Deep-Water Contourite Systems: Modern Drifts and Ancient Series, Seismic and Sedimentary Characteristics*, edited by D. A. V. Stow et al., *Mem. Geol. Soc. London*, *22*, 353–371.

Reynolds, J. M. (1981), The distribution of mean annual temperatures in the Antarctic Peninsula, *Br. Antarct. Surv. Bull.*, *54*, 123–133.

Rocchi, S., P. Armienti, M. D'Orazio, S. Tonarini, J. R. Wijbrans, and G. Di Vincenzo (2002), Cenozoic magmatism in the western Ross Embayment: Role of mantle plume versus plate dynamics in the development of the West Antarctic Rift System, *J. Geophys. Res.*, *107*(B9), 2195, doi:10.1029/2001JB000515.

Rodrigues, E. A., R. E. Houtz, J. L. LaBrecque, and D. A. Drewry (1986), Total sediment thickness, south; total sediment thickness, northwest; total sediment thickness, northeast, in *South Atlantic Ocean and Adjacent Antarctic Continental Margin*, *Reg. Atlas. Ser.*, vol. 13, p. 6, Mar. Sci. Int., Woods Hole, Mass.

Scheuer, C., K. Gohl, R. D. Larter, M. Rebesco, and G. Udintsev (2006a), Variability in Cenozoic sedimentation along the continental rise of the Bellingshausen Sea, West Antarctica, *Mar. Geol.*, *227*, 279–298.

Scheuer, C., K. Gohl, and G. Udintsev (2006b), Bottom-current control on sedimentation in the western Bellingshausen Sea, West Antarctica, *Geo Mar. Lett.*, *26*, 90–101, doi:10.1007/S00367-006-0019-1.

Shapiro, N. M., and M. H. Ritzwoller (2004), Inferring surface heat flux distributions guided by a global seismic model: Particular application to Antarctica, *Earth Planet. Sci. Lett.*, *223*, 1–2, 213–224.

Sijp, W., and M. H. England (2004), Effect of the Drake Passage throughflow on global climate, *J. Phys. Oceanogr.*, *34*, 1254–1266.

Smith, W. H. F., and D. T. Sandwell (1997), Global seafloor topography from satellite altimetry and ship depth soundings, *Science*, *277*, 1956–1961.

Stein, C., and S. Stein (1992), A model for the global variation in oceanic depth and heat flow with lithospheric age, *Nature*, *359*, 123–128.

Sykes, T. J. S. (1996), A correction for sediment load upon the ocean floor: Uniform versus varying sediment density estimations-implications for isostatic correction, *Mar. Geol.*, *133*, 35–49.

Sykes, T. J. S., J.-Y. Royer, A. T. S. Ramsay, and R. B. Kidd (1998), Southern Hemisphere palaeobathymetry, in *Geological Evolution of Ocean Basins: Results From the Ocean Drilling Program*, edited by A. Cramp et al., *Geol. Soc. Spec. Publ.*, *131*, 3–42.

Tomlinson, J. S., C. J. Pudsey, R. A. Livermore, R. D. Larter, and P. F. Barker (1992), Long-range sidescan sonar (GLORIA) survey of the Antarctic Peninsula Pacific margin, in *Recent Progress in Antarctic Earth Science*, edited by Y. Yoshida, K. Kaminuma, and K. Shiraishi, pp. 423–429, Terra Sci., Tokyo.

Tucholke, B. E., and R. E. Houtz (1976), Sedimentary framework of the Bellingshausen Basin from seismic profile data, *Initial Rep. Deep Sea Drill. Proj.*, *35*, 197–227.

Vaughan, D. G., A. M. Smith, H. F. J. Corr, A. Jenkins, C. R. Bentley, M. D. Stenoien, S. S. Jacobs, T. B. Kellog, E. Rignot, and B. K. Lucchitta (2001), A review of Pine Island Glacier, West Antarctica: Hypotheses of instability vs. observations of change, in *The West Antarctic Ice Sheet: Behavior and Environment*, *Antarct. Res. Ser.*, vol. 77, edited by R. B. Alley and R. A. Bindschadler, pp. 237–256, AGU, Washington, D. C.

Volpi, V., A. Camerlenghi, T. Moerz, P. Corubolo, M. Rebesco, and U. Tinivella (2001), Data report: Physical properties relevant to seismic stratigraphic studies, continental rise sites 1095, 1096, and 1101, ODP Leg 178, Antarctic Peninsula, in *Proc. Ocean Drill. Program Sci. Results* [CD-ROM], *178*, 1–40.

Wessel, P., and W. H. F. Smith (2004), The Generic Mapping Tool (GMT), version 3.4.5, technical reference and cookbook, report, NOAA, Silver Spring, Md.

Yamaguchi, K., Y. Tamura, I. Mizukoshi, and T. Tsuru (1988), Preliminary report of geophysical and geological surveys in the Amundsen Sea, West Antarctica, *Proc. NIPR Symp. Antarct. Geosci.*, *2*, 55–67.